

Magnon Nonlinear Hall Effect in 2D Antiferromagnetic Insulators

Jinyang Ni,^{1,*} Yuanjun Jin,² and Guoqing Chang^{1,†}

¹*Division of Physics and Applied Physics, School of Physics and Mathematical Sciences, Nanyang Technological University, Singapore 637731, Singapore.*

²*Guangdong Basic Research Center of Excellence for Structure and Fundamental Interactions of Matter, Guangdong Provincial Key Laboratory of Quantum Engineering and Quantum Materials, School of Physics, South China Normal University, Guangzhou 510006, China.*

Exploring antiferromagnetic (AFM) insulators has long been challenging due to their zero spontaneous magnetization and stable insulating state, with this challenge being even more pronounced in the 2D limit. In this letter, we propose the magnon nonlinear Hall effect, a second-order thermal Hall response of collective spin excitations in ordered magnets, as a novel approach to investigate 2D AFM insulators. We demonstrate that in layered honeycomb antiferromagnets, the nonlinear thermal Hall effect of magnons, intrinsically coupled to the magnetic order, can be induced and manipulated by a slight external-field perturbation, in contrast to the fermions or phonons. This coupling also gives rise to an intriguing magnetic-layer dependence of magnon nonlinear Hall response that is absent in the linear regime. For instance, in *G*-type AFM multilayers, this effect is allowed in odd layers but forbidden in even layers. Moreover, in odd layers, the magnon nonlinear Hall response is suppressed by the AFM interlayer coupling, with the strength decreasing as the layer numbers increases. The remarkable tunability and magnetic-dependent characteristics address the limitations of weak responses in AFM insulators, shedding light on 2D AFM spintronics.

Introduction. The realm of condensed matter physics has long been captivated by the complex interactions of electron spins in magnetic materials[1–5]. Among these, antiferromagnets stand out due to its fundamental physical perspective[6–9]. However, the inherent zero net magnetization of antiferromagnets significantly hinders their probing and applications[8]. This challenge is amplified in recently discovered two-dimensional (2D) van-der-Waals (vdW) antiferromagnetic (AFM) insulators, typified as the family of MPX_3 ($M = V, Mn, Fe, Co, Ni; X = S, Se, Te$)[10–16]. The difficulty primarily arises from the limitations of traditional measurement methods for atomic thick antiferromagnets[17–19] and the diverse stacking configurations of these materials[20–22]. Additionally, AFM insulators generally exhibit robustness against to the external fields, resulting in a markedly weak response in electronic or spin transport under such perturbations[8, 9].

Recent advances in magnon-based phenomena[23–33], particularly the thermal Hall effect of magnons[23, 34–38], have opened new avenues for the study of 2D magnetic insulators. For instance, the linear spin Nernst effect (SNE) of magnons observed in layered honeycomb antiferromagnets (*h*AFM)[39–41], originates from the Dzyaloshinsky-Moriya interaction (DMI)[42, 43]. However, the DMI, an intrinsic spin-orbit coupling (SOC) effect, is typically weak in *3d* magnetic ions[44] and cannot be readily manipulated by external fields. Moreover, in antiferromagnets, the linear SNE is independence from both the magnetic structure and layer number[39, 40, 45], which significantly restricts the ability to capture its magnetic characteristics. Overall, it's urgent to develop a comprehensive approach that both address these limitations and effectively capture the unique properties of 2D AFM insulators.

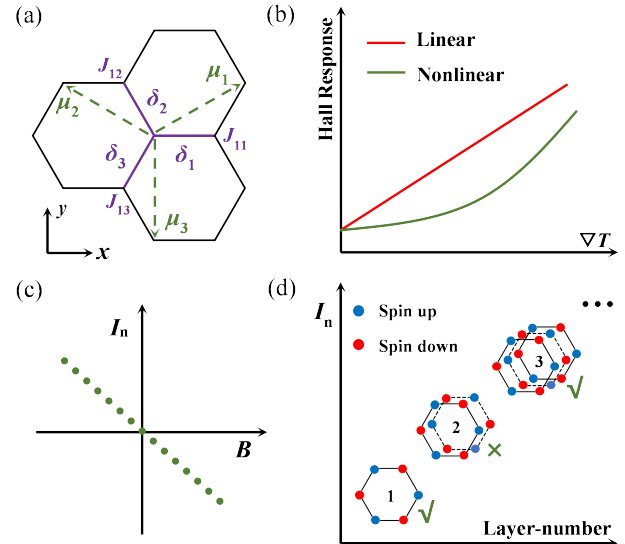


FIG. 1. (a) Schematic of monolayer honeycomb magnets, where δ_i and μ_i connects NN and NNN sites, respectively. (b) Illustration of linear (red line) and nonlinear (green line) magnon Hall effect. (c) Reversal of magnon nonlinear Hall response by B . (d) Layer-number selective rule for nonlinear Hall effect in *G*-type *h*AFM, where each layer adopts an easy-axis Néel order and is coupled to adjacent layers via AFM coupling.

In this letter, we unveil distinct characteristics of magnon nonlinear Hall effect that can effectively address the limitations associated with 2D AFM insulators. Confirmed by the symmetry analysis, we show that the intrinsic nonlinear transversal heat current can be generated by nonzero extended Berry curvature dipole (BCD) of magnons, which is feasible in the magnetic groups with

broken effective inversion symmetry \mathcal{P} and is independent of SOC. By applying a finite Zeeman field \mathcal{B} , a giant net nonlinear thermal Hall response can be induced and manipulated, which is distinct from the known nonlinear Hall effects observed in fermions or phonons[46, 47]. The coupling to the magnetic order also leads to an intriguing layer-number selection rule for magnon nonlinear Hall effect that is absent in the linear regime; for instance, in G -type multilayers h AFM as depicted in Fig.1(d), this nonlinear Hall effect is allowed in odd layers but forbidden in even layers. Additionally, the strength of magnon nonlinear Hall decreases as the layer number increases. Above theoretical proposal is validated by the numerical results of layered vdW AFM insulators VPX_3 .

Monolayer. Our discussion begins with the monolayer honeycomb antiferromagnet (m AFM), for which the spin model can be expressed as:

$$\begin{aligned} \hat{\mathcal{H}}_m = & \mathcal{J}_1 \sum_{\langle i,j \rangle} \mathcal{S}_i \cdot \mathcal{S}_j + \mathcal{D}_z \sum_{\langle i,j \rangle'} \boldsymbol{\nu}_{ij} \cdot (\mathcal{S}_i \times \mathcal{S}_j) \\ & + \sum_i \mathcal{K} (\mathcal{S}_i^z)^2 - \mathcal{B} \sum_i \mathcal{S}_i^z. \end{aligned} \quad (1)$$

Here, the first term is AFM exchange with $\mathcal{J}_1 > 0$ for nearest-neighbor (NN) magnetic moments on honeycomb lattice. The second term is next-nearest-neighbor (NNN) out-of-plane DM interaction \mathcal{D}_z [42, 43], where the direction is defined as $\boldsymbol{\nu}_{ij} = 2\sqrt{3}\boldsymbol{\delta}_i \times \boldsymbol{\delta}_j = \pm\mathbf{z}$, with $\boldsymbol{\delta}_i$ being NN linking vectors, as shown in Fig.1(a). The third term represents the easy-axis single ion anisotropy (SIA) with $\mathcal{K} < 0$. For simplicity, the external Zeeman field \mathcal{B} is applied along z -axis. The following discussion is restricted to $|\mathcal{J}_1| \gg |\mathcal{D}_z|$ and $2|\mathcal{K}|S > |\mathcal{B}|$, ensuring that the magnetic ground state remains in the collinear Néel order, as detailed in the Supplemental Material (SM)[48].

The linear spin wave model in Eq.(1) can be solved by employing Holstein-Primakoff (HP) transformation[49], $\mathcal{S}_{i,\uparrow}^+ \approx \sqrt{2S}\hat{a}_i$, $\mathcal{S}_{i,\downarrow}^+ \approx \sqrt{2S}\hat{b}_i^\dagger$, $\mathcal{S}_{i,\uparrow}^z = S - \hat{a}_i^\dagger \hat{a}_i$ and $\mathcal{S}_{i,\downarrow}^z = \hat{b}_i^\dagger \hat{b}_i - S$. Upon Fourier transformation, the Hamiltonian can be expressed in the spinor basis $\psi_k^\dagger \equiv (\hat{a}_k^\dagger, \hat{b}_{-k}, \hat{a}_{-k}, \hat{b}_k^\dagger)$ as $\hat{\mathcal{H}}_m = \sum_k \psi_k^\dagger \hat{\mathcal{H}}_{mk} \psi_k$. Neglecting the zero-point energy and assuming $S = 1$, $\hat{\mathcal{H}}_k$ reads as,

$$\hat{\mathcal{H}}_{mk} = \lambda I + \begin{pmatrix} f_k + \mathcal{B} & \gamma_k & 0 & 0 \\ \gamma_k^\dagger & -f_k - \mathcal{B} & 0 & 0 \\ 0 & 0 & \mathcal{B} - f_k & \gamma_k^\dagger \\ 0 & 0 & \gamma_k & f_k - \mathcal{B} \end{pmatrix}. \quad (2)$$

where $\lambda = -3\mathcal{J}_1 - 2\mathcal{K}$, $\gamma_k = \mathcal{J}_1 \sum_i \exp(i\mathbf{k} \cdot \boldsymbol{\delta}_i)$, and $f_k = \mathcal{D}_z \sum_{i \in \text{odd}} 2\sin(\mathbf{k} \cdot \boldsymbol{\mu}_i)$ with $\boldsymbol{\mu}_i$ the vectors linking NNN sites as shown in Fig.1(a).

Using the Bogoliubov transformation[48, 50, 51], we can diagonalize Eq.(2), with the corresponding analytical solutions given by,

$$\epsilon_{\pm} = \epsilon_0 + f_k \pm \mathcal{B}, \quad \Psi_{\pm}^\dagger = \frac{\sqrt{2}}{2} \begin{pmatrix} -\lambda \pm \epsilon_0 \\ \gamma_k (\gamma_k^\dagger), 1 \end{pmatrix}, \quad (3)$$

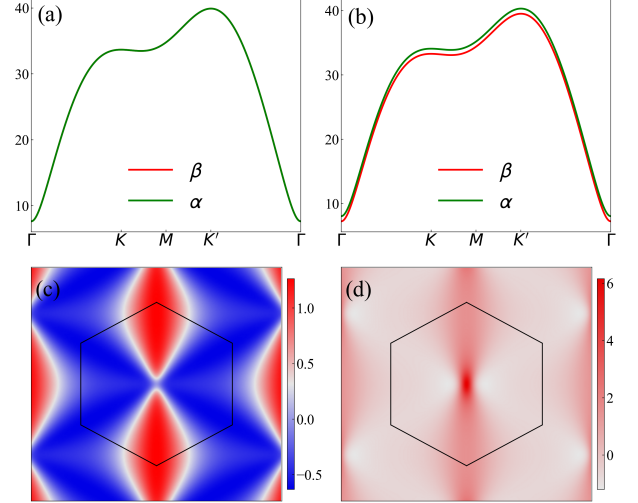


FIG. 2. (a)-(b) Magnon bands (units of meV) of monolayer $VPTe_3$ with (a) $\mathcal{B} = 0$ and (b) $\mathcal{B} = -0.4$ meV. Clearly, the bands both gap at Γ -point with the gap being equal to $2S\sqrt{|\mathcal{K}|^2 - 4\mathcal{K}\mathcal{J}_1}$. (c) Corresponding extended BCD of magnons (minor band) without strain, (d) with 3% uniaxial stretching strain.

where \pm represent the α and β mode, respectively, and $\epsilon_0 = \sqrt{\lambda^2 - |\gamma_k|^2}$. Clearly, normalized wavefunction Ψ is independent of \mathcal{D}_z and \mathcal{B} ; hence, Berry curvature can be determined as follows

$$\Omega_{\pm}^z = \pm \frac{\lambda}{2\epsilon_0^3} (\nabla \text{Re} \gamma_k \times \nabla \text{Im} \gamma_k). \quad (4)$$

This can be explained by the symmetry argument of magnetic group[52], where the Néel order naturally breaks the inversion symmetry \mathcal{P} [52], leading to $\Omega(k) = -\Omega(-k)$. Thus, the nonzero Ω emerges when \mathcal{B} and \mathcal{D}_z are both zero. In this scenario, two degenerate magnon modes of m AFM, α and β , are odd with respect to \mathbf{k} , characterized by spin angular value $\langle S^z \rangle$ with chirality ± 1 .

While the \mathcal{D}_z preserves two-fold degeneracy, it breaks $C_2\mathcal{T}$ symmetry, where C_2 denotes the π rotation along x/y -axis, leading to $\epsilon(k) \neq \epsilon(-k)$ as shown in Fig.2(a). This correction induced by the \mathcal{D}_z leads to the emergence of spin-Hall like magnon current, known as linear magnon SNE[39, 40, 45]. In addition to linear Hall response, the odd nature of $\Omega(k)$, arising from the broken inversion symmetry \mathcal{P} , gives rise to a nonlinear Hall response[46]. By solving the Boltzmann equation, as detailed in SM.V[48], we derived the nonlinear spin-Nernst conductivity I^s and thermal Hall conductivity I^ϵ of magnons up to second order, which are given by

$$\begin{aligned} I_a^s & \approx \frac{\varepsilon_{abc}}{V\hbar^2 T} \sum_{n,k} c_1(\rho) \langle S_n^z \rangle \partial_{k_b} [\Omega_{n,k}^c \epsilon_{n,k}], \\ I_a^\epsilon & \approx \frac{2\varepsilon_{abc}}{V\hbar^2 T} \sum_{n,k} c_1(\rho) \epsilon_{n,k} \partial_{k_b} [\Omega_{n,k}^c \epsilon_{n,k}], \end{aligned} \quad (5)$$

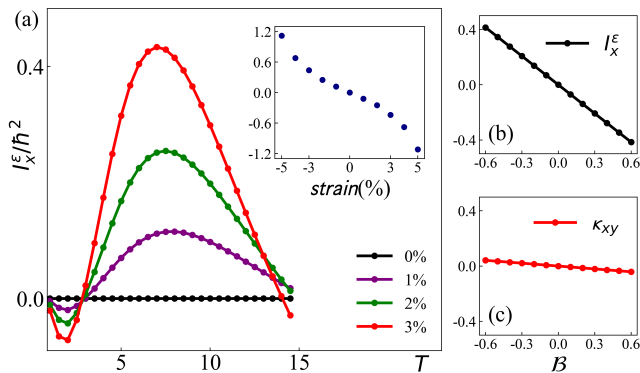


FIG. 3. Thermal Hall response of monolayer VPTe₃. (a) I_x^ϵ as a function of temperature T . The inset figure is I_x^ϵ as a function of uniaxial strain along x -axis. (b) Nonlinear thermal Hall conductivity I_x^ϵ at T_N as the function of \mathcal{B} . (c) Linear thermal Hall conductivity κ_{xy} versus \mathcal{B} .

where V is volume, ϵ_{abc} is Levi-Civita symbol with $abc = xyz$ and $c_1(\rho) = \int_0^\rho \log(1 + \rho^{-1}) d\rho$ with ρ being Boltzmann distributions for bosons. In 2D case, $c = z$, indicating that the nonlinear transverse current can emerge along y -axis when applying temperature gradient along x -axis. Obviously, I^s and I^ϵ both depend on $\partial_{k_y} [\Omega_{n,k} \epsilon_{n,k}] = [\Omega_{n,k} v_y^\epsilon + \epsilon_{n,k} v_y^\Omega]$, analogous to the BCD defined in fermions[46], which is referred to as the extended BCD of magnons[53, 54]. In contrast, the I^s is associated with the expected value of $\langle S_n^z \rangle$, while I^ϵ pertains to the ϵ_n of magnons.

As shown Fig.2(c), the extended BCD distribution of α mode is even with respect to \mathbf{k} . However, since the \mathcal{C}_{3z} symmetry can transform k_m to k_μ and k_ν in k -space, when $\mathcal{D}_z = 0$, it allows

$$v_{y,k_m}^{\epsilon/\Omega} + v_{y,k_\mu}^{\epsilon/\Omega} + v_{y,k_\nu}^{\epsilon/\Omega} = 0, \quad (6)$$

indicating Eq.(5) remains zero. The \mathcal{C}_{3z} symmetry can be broken by disrupting the invariance among the NN spin exchange interactions \mathcal{J}_{11} , \mathcal{J}_{12} and \mathcal{J}_{13} , as demonstrated by application of uniaxial strain, illustrated in Fig.1(a). Consequently, the nonzero summation of velocity permits the emergence of a nonlinear transverse heat current, which is perpendicular to the applied temperature gradient and parallel to the direction of the uniaxial strain. The emergence of \mathcal{D}_z can also lead to nonzero values of Eq.(5), with details provided in the Fig.S7[48, 55]. When $\mathcal{B} = 0$, the degeneracy of modes with opposite chirality prevents the generation of the net transverse heat current but allow for the nonlinear SNE[53, 54].

Since the parity of each magnon mode is locked by $\langle S^z \rangle$, which is also coupled to \mathcal{B} , such that a finite \mathcal{B} can break this degeneracy. As shown in Fig.2(b), when $\mathcal{B} > 0$, α mode is higher in energy than the β mode, resulting in $\sum_k \partial_{k_y} [\Omega_\alpha^z \epsilon_\alpha + \Omega_\beta^z \epsilon_\beta] > 0$. This indicates that switching the \mathcal{B} naturally flips the sign of I_x^ϵ , which is

fundamentally different from the known nonlinear Hall effect observed in fermions[46, 56] or phonons[47, 57], as the latter is independent of the magnetic field. Note that the role of applied \mathcal{B} is merely to lift the degeneracy of magnon modes, with its strength being much smaller than SIA, thereby preserving the advantage of AFM magnons with photonlike linear dispersion Γ -point, reaching THz frequency [8, 58].

Above theoretical proposal can be readily verified in various 2D h AFM, such as the transition metal phosphorus trichalcogenide VPX₃ with $X = S, Se, Te$. Recent experiments[11, 16] have verified the stability and magnetic ground state of bulk VPX₃, where honeycomb magnetic lattice within each layer, composed of V^{+2} magnetic ion with $S = 3/2$, exhibits an easy-axis Néel order below the Néel temperature T_N . Using energy mapping DFT calculations[48, 59–63], we constructed the effective spin Hamiltonian of monolayer VPTe₃, finding $\mathcal{J}_1 = 12$ meV, $\mathcal{D}_z = 0.6$ meV and $\mathcal{K} = -0.4$ meV. When a slight uniaxial strain is applied along x -axis, \mathcal{J}_{11} and \mathcal{J}_{12} remain almost unchanged, while \mathcal{J}_{13} change rapidly due to their strong spin-lattice coupling[62]. Specifically, $\mathcal{J}_{13} \approx 0.5\mathcal{J}_{11}$ with 3% uniaxial stretching strain. The main results of monolayer VPS₃ and VPSe₃ are shown in SM.VI[48], which are consistent with VPTe₃.

Fig.3(a) shows the dependence of I_x^ϵ on temperature T with different uniaxial strain along x -axis, ranging from 0% to 3%, in monolayer VPTe₃. Clearly, a slight perturbation induced by applied strain can generate a giant nonlinear thermal Hall response under the \mathcal{B} , which starts from zero at low T and peaks around T_N . Since extended BCD is odd under \mathcal{P} but even under \mathcal{T} , reversing the chirality of uniaxial strain can flip the sign of I_x^ϵ . This behavior is different from the case of applying \mathcal{B} , which flips the sign of I^ϵ by altering the position of magnon modes, as shown in Fig.3(a)-(b). Compared to the substantial nonlinear response, the linear thermal Hall response induced by the band splitting and nonzero \mathcal{D}_z is negligible, as depicted in Fig.3(c). Therefore, the nonlinear response is dominant contribution to the thermal Hall effect in strained m AFM under \mathcal{B} .

Bilayer. The spin model of bilayer honeycomb antiferromagnet (b AFM) can read as $\hat{\mathcal{H}}_b = \hat{\mathcal{H}}_m + \hat{\mathcal{H}}_c$, where $\hat{\mathcal{H}}_c$ is interlayer coupling term. Similar to m AFM, the momentum-space magnon Hamiltonian of b AFM $\hat{\mathcal{H}}_{bk}$ can split into two blocks. The first block, $\hat{\mathcal{H}}_{bk}^I$, is described by spinor basis $\psi_{I,k}^\dagger \equiv (\hat{a}_{1,k}^\dagger, \hat{b}_{2,k}^\dagger, \hat{b}_{1,-k}, \hat{a}_{2,-k})$, where $\hat{a}_{1(2),k}^\dagger$ creates the a magnon in first(second) layer at k -point. $\hat{\mathcal{H}}_{bk}^I$ read as

$$\hat{\mathcal{H}}_{bk}^I = \lambda I + \begin{pmatrix} f_k + \mathcal{B} & 0 & \gamma_k & \mathcal{J}_c \\ 0 & \mathcal{B} - f_k & \mathcal{J}_c & \gamma_k^\dagger \\ \gamma_k^\dagger & \mathcal{J}_c & -f_k - \mathcal{B} & 0 \\ \mathcal{J}_c & \gamma_k & 0 & f_k - \mathcal{B} \end{pmatrix} \quad (7)$$

where $\mathcal{J}_c > 0$ represents AFM interlayer coupling. The

second block of Hamiltonian described by $\psi_{II,k}^\dagger$ can be obtained by $\gamma_k \rightarrow \gamma_{-k}$, $f_k \rightarrow f_{-k}$ and $\mathcal{B} \rightarrow -\mathcal{B}$ in Eq.(7). By performing Bogoliubov transformation, eigenvalues can be derived as

$$\begin{aligned} \epsilon_{\pm}^1 &= \pm \mathcal{B} + \sqrt{\epsilon_c^2 + \epsilon_0^2 - 2\sqrt{\lambda^2 f_k^2 - |\gamma_k|^2} \epsilon_c^2} \\ \epsilon_{\pm}^2 &= \pm \mathcal{B} + \sqrt{\epsilon_c^2 + \epsilon_0^2 + 2\sqrt{\lambda^2 f_k^2 - |\gamma_k|^2} \epsilon_c^2} \end{aligned} \quad (8)$$

with $\epsilon_c^2 = f_k^2 - \mathcal{J}_c^2$. The corresponding eigenvectors are functions of $\mathcal{D}_z f_k$, \mathcal{J}_c and γ_k , but are independent under \mathcal{B} , as shown in SM.III[48]. Since the magnon Hamiltonian of *b*AFM is preserved by $\mathcal{M}_z \mathcal{T}$ and \mathcal{P} , $\Omega(k) = 0$ when $\mathcal{D}_z = 0$, where \mathcal{M}_z is mirror reflection of *xy* plane.

The \mathcal{D}_z term can break the Dirac-cones of magnon bands at K-points, as shown in Fig.S3[48], while the two-fold degenerate state remains unchanged, with each state characterized by the $\langle S^z \rangle$ [48]. When $\mathcal{D}_z > 0$, the $\Omega(k)$ of one mode in minor magnon band illustrated in Fig.4(a), exhibits monopole type located at the M-points, which is opposite to another degenerate mode due to the effective \mathcal{T} . This even nature of $\Omega(k)$ ensures that each magnon mode carries nonzero linear transverse heat current, but the degeneracy of modes prevents the generation of a net heat current under the applied temperature gradient. Furthermore, in *b*AFM with $\mathcal{J}_c > 0$, $\mathcal{M}_z \mathcal{T}$ and \mathcal{P} allows for the energy bands satisfying $\epsilon(k) = \epsilon(-k)$, indicating that the magnon nonlinear Hall response is forbidden. This result remains unchanged even when breaking \mathcal{C}_{3z} symmetry or applying \mathcal{B} .

This layer dependence of magnon nonlinear Hall effect can easily extend to arbitrary-even-layers or bulk phase *h*AFM with Néel order, as \mathcal{J}_c can be replaced by $2\mathcal{J}_c \cos k_z$ in the magnon Hamiltonian for bulk phase. For even-layer *h*AFM with AFM interlayer coupling, referred to as *G*-type *h*AFM, the $\mathcal{M}_z \mathcal{T}$ and \mathcal{P} are preserved[52]. In this case, the nonzero Berry curvature of magnons can be achieved by breaking $\mathcal{C}_2 \mathcal{T}$ via \mathcal{D}_z . This leads to magnon bands and corresponding Berry curvature satisfy $\epsilon(k) = \epsilon(-k)$ and $\Omega(k) = \Omega(-k)$. Thereby, extended BCD of each band is odd with respect to \mathbf{k} , such that the magnon nonlinear Hall response is forbidden. Conversely, as illustrated in Fig.4(b), nonlinear magnon Hall response can emerge in even-layer *h*AFM with ferromagnetic (FM) coupling ($\mathcal{J}_c < 0$), as the \mathcal{P} and $\mathcal{M}_z \mathcal{T}$ are broken. This feature, intrinsically linked to the weak interlayer coupling, will be crucial for probing the magnetic ground state of few-layers AFM insulators with weak interlayer coupling.

Trilayer. Similarly, we can obtain the magnon band of trilayer *h*AFM with Néel order (*t*AFM), which is two-fold degenerate when $\mathcal{B} = 0$, as shown in Fig.S4[48]. Notably, the eigenvectors of first and third band are function of f_k and the corresponding $\Omega(k)$ is even with respect to \mathbf{k} , indicating there is no contribution to the nonlinear Hall

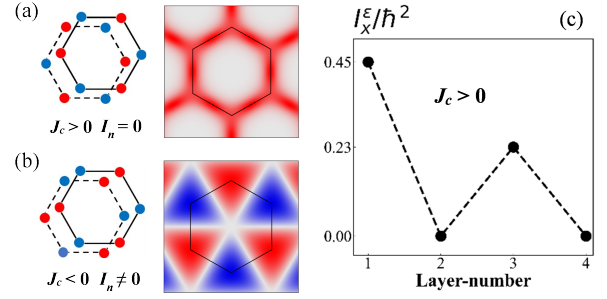


FIG. 4. The Ω of minor magnon band in *b*AFM, (a) with AFM interlayer coupling $\mathcal{J}_c > 0$ and (b) FM interlayer coupling $\mathcal{J}_c < 0$. (c) Nonlinear thermal Hall conductivity I_x^ϵ at T_N as a function of layer-number. Here, $\mathcal{J}_c \approx 0.2 \mathcal{J}_1$, which is reasonable for layered vdW magnets. The applied external field is identical for both monolayer and multilayers.

response of magnons. The normalized eigenvalues and Berry curvature of second band are given by

$$\begin{aligned} \epsilon_{\pm} &= \sqrt{\lambda_t - |\gamma_k|^2} + f_k \pm \mathcal{B}, \\ \Omega_{\pm}^z &= \pm \frac{\lambda_t}{2\epsilon_t^3} (\nabla \text{Re} \gamma_k \times \nabla \text{Im} \gamma_k), \end{aligned} \quad (9)$$

where $\lambda_t = \mathcal{J}_c + \lambda$ and $\epsilon_t = \sqrt{\lambda_t^2 - |\gamma_k|^2}$. Compared with *m*AFM, the second band of *t*AFM also contributes to nonlinear Hall response; however, the corresponding $\Omega(k)$ and extended BCD is suppressed by \mathcal{J}_c . This feature results in an intriguing layer dependence of magnon nonlinear Hall effect in layered antiferromagnets as shown in Fig.4(c). Beyond the odd-even layer selective rule, this nonlinear effect is suppressed by the AFM interlayer coupling, with its strength decreasing as the layer number increases. In contrast, linear thermal Hall effect or SNE of magnons generally show a positive relationship with the layer number[40, 45].

Discussion and summary. According to the above symmetry analysis, magnon nonlinear Hall response is naturally forbidden in ferromagnets due to their \mathcal{P} being preserved[52], as detailed in SM.II-III[48]. For collinear *h*AFM with zigzag or stripe order, the effective \mathcal{P} , which combines the inversion symmetry and translational symmetry, is preserved, resulting in the magnon nonlinear Hall response vanishes[48]. This magnetic-symmetry-constrained rule for nonlinear Hall effect of magnons contrasts with the linear thermal Hall effect, which requires only that $\mathcal{C}_2 \mathcal{T}$ to be broken by \mathcal{D}_z [38, 64]. Therefore, magnon nonlinear Hall effect is particularly advantageous for probing the magnetic structure of antiferromagnets, such as identifying the type of interlayer coupling or the spin order within each layer.

A similar magnetic associated nonlinear transport effect has also been recently observed in electrons, as seen in even-layer MnBi_2Te_4 [65, 66] and monolayer MnS [67]. This newly discovered nonlinear Hall effect of electrons is induced by the quantum metric, real part of quan-

tum geometry tensor of electron Bloch wavefunctions[65–67]. Despite of this, the nonlinear Hall effect of magnons proposed here exhibits several distinctions from the electrons. Firstly, nonlinear Hall effect in electrons require a nonzero fermi-surface or a narrow band gap, but magnons can overcome this limitation. Secondly, nonlinear Hall effect of electrons is independent of external fields, whereas magnons is highly tunable by the external magnetic-field \mathcal{B} or applied strain.

In summary, we have theoretically investigated the magnon nonlinear Hall effect in 2D vdW AFM insulators, revealing their remarkable tunability and intriguing magnetic-dependent characteristic. Our findings not only shed light on potential applications of AFM spintronics, but also provide an entirely new approach for detecting the magnetic order in 2D vdW magnetic insulators.

We acknowledge useful discussions with Dr.Du Quanchao, Dr.Hou Tao, Dr.Rohit Mukherjee and Prof.Arijit Kundu. This work at Nanyang Technological University was financially supported by grants from the National Research Foundation, Singapore under its Fellowship Award (NRF-NRFF13-2021-0010), the Nanyang Technological University startup grant (NTUSUG). We gratefully acknowledge the ASPIRE2A platform at Singapore National Supercomputing Centre (NSCC) for their generous allocation of CPU time.

* jinyang.ni@ntu.edu.sg

† guoqing.chang@ntu.edu.sg

- [1] P. W. Anderson, *Phys. Rev.* **79**, 350 (1950).
- [2] P. W. Anderson, *Science* **177**, 393 (1972).
- [3] B. Huang, G. Clark, E. Navarro-Moratalla, D. R. Klein, R. Cheng, K. L. Seyler, D. Zhong, E. Schmidgall, M. A. McGuire, D. H. Cobden, *et al.*, *Nature* **546**, 270 (2017).
- [4] C. Gong, L. Li, Z. Li, H. Ji, A. Stern, Y. Xia, T. Cao, W. Bao, C. Wang, Y. Wang, *et al.*, *Nature* **546**, 265 (2017).
- [5] A. Szilva, Y. Kvashnin, E. A. Stepanov, L. Nordström, O. Eriksson, A. I. Lichtenstein, and M. I. Katsnelson, *Rev. Mod. Phys.* **95**, 035004 (2023).
- [6] L. Néel, *Ann. Phys.* **12**, 137 (1948).
- [7] F. Keffer and C. Kittel, *Phys. Rev.* **85**, 329 (1952).
- [8] V. Baltz, A. Manchon, M. Tsoi, T. Moriyama, T. Ono, and Y. Tserkovnyak, *Rev. Mod. Phys.* **90**, 015005 (2018).
- [9] T. Jungwirth, X. Marti, P. Wadley, and J. Wunderlich, *Nat. Nanotechnol.* **11**, 231 (2016).
- [10] K. Du, X. Wang, Y. Liu, P. Hu, M. I. B. Utama, C. K. Gan, Q. Xiong, and C. Kloc, *ACS Nano* **10**, 1738 (2016).
- [11] F. Wang, T. A. Shifa, P. Yu, P. He, Y. Liu, F. Wang, Z. Wang, X. Zhan, X. Lou, F. Xia, *et al.*, *Adv. Funct. Mater.* **28**, 1802151 (2018).
- [12] Z. Ni, H. Zhang, D. A. Hopper, A. V. Haglund, N. Huang, D. Jariwala, L. C. Bassett, D. G. Mandrus, E. J. Mele, C. L. Kane, *et al.*, *Phys. Rev. Lett.* **127**, 187201 (2021).
- [13] K. Kim, S. Y. Lim, J.-U. Lee, S. Lee, T. Y. Kim, K. Park, G. S. Jeon, C.-H. Park, J.-G. Park, and H. Cheong, *Nat. Commun.* **10**, 345 (2019).
- [14] T. Klaproth, S. Aswartham, Y. Shemerliuk, S. Selzer, O. Janson, J. van den Brink, B. Büchner, M. Knupfer, S. Pazek, D. Mikhailova, *et al.*, *Phys. Rev. Lett.* **131**, 256504 (2023).
- [15] Z. Ni, A. Haglund, H. Wang, B. Xu, C. Bernhard, D. Mandrus, X. Qian, E. Mele, C. Kane, and L. Wu, *Nat. Nanotechnol.* **16**, 782 (2021).
- [16] C. Liu, Z. Li, J. Hu, H. Duan, C. Wang, L. Cai, S. Feng, Y. Wang, R. Liu, D. Hou, *et al.*, *Adv. Mater.* **35**, 2300247 (2023).
- [17] M. Gibertini, M. Koperski, A. F. Morpurgo, and K. S. Novoselov, *Nat. Nanotechnol.* **14**, 408 (2019).
- [18] K. F. Mak, J. Shan, and D. C. Ralph, *Nat. Rev. Phys.* **1**, 646 (2019).
- [19] B. Huang, M. A. McGuire, A. F. May, D. Xiao, P. Jarillo-Herrero, and X. Xu, *Nat. Mater.* **19**, 1276 (2020).
- [20] H. Chu, C. J. Roh, J. O. Island, C. Li, S. Lee, J. Chen, J.-G. Park, A. F. Young, J. S. Lee, and D. Hsieh, *Phys. Rev. Lett.* **124**, 027601 (2020).
- [21] N. Sivadas, S. Okamoto, X. Xu, C. J. Fennie, and D. Xiao, *Nano Lett.* **18**, 7658 (2018).
- [22] P. Jiang, C. Wang, D. Chen, Z. Zhong, Z. Yuan, Z.-Y. Lu, and W. Ji, *Phys. Rev. B* **99**, 144401 (2019).
- [23] Y. Onose, T. Ideue, H. Katsura, Y. Shiomi, N. Nagaosa, and Y. Tokura, *Science* **329**, 297 (2010).
- [24] P. A. McClarty, *Annu. Rev. Condens. Matter Phys.* **13**, 171 (2022).
- [25] A. V. Chumak, V. I. Vasyuchka, A. A. Serga, and B. Hillebrands, *Nat. Phys.* **11**, 453 (2015).
- [26] S. Bao, J. Wang, W. Wang, Z. Cai, S. Li, Z. Ma, D. Wang, K. Ran, Z.-Y. Dong, D. Abernathy, *et al.*, *Nat. Commun.* **9**, 2591 (2018).
- [27] W. Yao, C. Li, L. Wang, S. Xue, Y. Dan, K. Iida, K. Kamazawa, K. Li, C. Fang, and Y. Li, *Nat. Phys.* **14**, 1011 (2018).
- [28] A. Mook, K. Plekhanov, J. Klinovaja, and D. Loss, *Phys. Rev. X* **11**, 021061 (2021).
- [29] J. Li, C. B. Wilson, R. Cheng, M. Lohmann, M. Kavand, W. Yuan, M. Aldosary, N. Agladze, P. Wei, M. S. Sherwin, *et al.*, *Nature* **578**, 70 (2020).
- [30] K. Li, C. Li, J. Hu, Y. Li, and C. Fang, *Phys. Rev. Lett.* **119**, 247202 (2017).
- [31] L. Chen, J.-H. Chung, B. Gao, T. Chen, M. B. Stone, A. I. Kolesnikov, Q. Huang, and P. Dai, *Phys. Rev. X* **8**, 041028 (2018).
- [32] J. Cenker, B. Huang, N. Suri, P. Thijssen, A. Miller, T. Song, T. Taniguchi, K. Watanabe, M. A. McGuire, D. Xiao, *et al.*, *Nat. Phys.* **17**, 20 (2021).
- [33] Z. Jin, X. Yao, Z. Wang, H. Yuan, Z. Zeng, W. Wang, Y. Cao, and P. Yan, *Phys. Rev. Lett.* **131**, 166704 (2023).
- [34] H. Katsura, N. Nagaosa, and P. A. Lee, *Phys. Rev. Lett.* **104**, 066403 (2010).
- [35] R. Matsumoto and S. Murakami, *Phys. Rev. Lett.* **106**, 197202 (2011).
- [36] R. Matsumoto, R. Shindou, and S. Murakami, *Phys. Rev. B* **89**, 054420 (2014).
- [37] X.-T. Zhang, Y. H. Gao, and G. Chen, *Phys. Rep.* **1070**, 1 (2024).
- [38] H. Zhang, C. Xu, C. Carnahan, M. Sretenovic, N. Suri, D. Xiao, and X. Ke, *Phys. Rev. Lett.* **127**, 247202 (2021).
- [39] R. Cheng, S. Okamoto, and D. Xiao, *Phys. Rev. Lett.* **117**, 217202 (2016).
- [40] V. A. Zyuzin and A. A. Kovalev, *Phys. Rev. Lett.* **117**, 217203 (2016).

- [41] Y. Shiomi, R. Takashima, and E. Saitoh, *Phys. Rev. B* **96**, 134425 (2017).
- [42] I. Dzyaloshinsky, *J. Phys. Chem. Solids* **4**, 241 (1958).
- [43] T. Moriya, *Phys. Rev.* **120**, 91 (1960).
- [44] D. I. Khomskii, *Transition Metal Compounds* (Cambridge University Press, 2014).
- [45] K. H. Lee, S. B. Chung, K. Park, and J.-G. Park, *Phys. Rev. B* **97**, 180401 (2018).
- [46] I. Sodemann and L. Fu, *Phys. Rev. Lett.* **115**, 216806 (2015).
- [47] W. Luo, J. Ji, P. Chen, Y. Xu, L. Zhang, H. Xiang, and L. Bellaiche, *Phys. Rev. B* **107**, L241107 (2023).
- [48] Supplemental Material includes I.Holstein-Primakoff (HP) transformation; II-III. Magnon model of layered honeycomb magnets; IV. Berry curvature of Magnons; V.Thermal transport of magnons; and VI. DFT calculations, Monte-Carlo simulations and numerical results of monolayer VPX_3 .
- [49] T. Holstein and H. Primakoff, *Phys. Rev.* **58**, 1098 (1940).
- [50] N. N. Bogoljubov, V. V. Tolmachov, and D. Širkov, *Fortschr. Phys.* **6**, 605 (1958).
- [51] J. Valatin, *Il Nuovo Cimento (1955-1965)* **7**, 843 (1958).
- [52] W. Brinkman and R. J. Elliott, *Proc. R. Soc. A* **294**, 343 (1966).
- [53] H. Kondo and Y. Akagi, *Phys. Rev. Res.* **4**, 013186 (2022).
- [54] R. Mukherjee, S. Verma, and A. Kundu, *Phys. Rev. B* **107**, 245426 (2023).
- [55] The strength of I_x^e induced by \mathcal{D}_z is approximately three orders of magnitude smaller than that induced by uniaxial strain. Additionally, the sign of I_x^e can be reversed by flipping the direction of \mathcal{B} .
- [56] Q. Ma, S.-Y. Xu, H. Shen, D. MacNeill, V. Fatemi, T.-R. Chang, A. M. Mier Valdivia, S. Wu, Z. Du, C.-H. Hsu, *et al.*, *Nature* **565**, 337 (2019).
- [57] H. Chen, Q. Wang, X. Feng, W. Wu, and L. Zhang, *Nano Lett.* **23**, 11266 (2023).
- [58] O. Gomonay, V. Baltz, A. Brataas, and Y. Tserkovnyak, *Nat. Phys.* **14**, 213 (2018).
- [59] J. P. Perdew, K. Burke, and M. Ernzerhof, *Phys. Rev. Lett.* **77**, 3865 (1996).
- [60] P. E. Blöchl, *Phys. Rev. B* **50**, 17953 (1994).
- [61] A. Liechtenstein, V. I. Anisimov, and J. Zaanen, *Phys. Rev. B* **52**, R5467 (1995).
- [62] H. Xiang, E. Kan, S.-H. Wei, M.-H. Whangbo, and X. Gong, *Phys. Rev. B* **84**, 224429 (2011).
- [63] H. Xiang, C. Lee, H.-J. Koo, X. Gong, and M.-H. Whangbo, *Dalton T.* **42**, 823 (2013).
- [64] S. Owerre, *J. Phys. Condens. Matter.* **28**, 386001 (2016).
- [65] N. Wang, D. Kaplan, Z. Zhang, T. Holder, N. Cao, A. Wang, X. Zhou, F. Zhou, Z. Jiang, C. Zhang, *et al.*, *Nature* **621**, 487 (2023).
- [66] A. Gao, Y.-F. Liu, J.-X. Qiu, B. Ghosh, T. V. Trevisan, Y. Onishi, C. Hu, T. Qian, H.-J. Tien, S.-W. Chen, *et al.*, *Science* **381**, 181 (2023).
- [67] J. Wang, H. Zeng, W. Duan, and H. Huang, *Phys. Rev. Lett.* **131**, 056401 (2023).